

Available online at www.sciencedirect.com**ScienceDirect**

Procedia Environmental Sciences 24 (2015) 266 – 276

Procedia
Environmental Sciences

The 1st International Symposium on LAPAN-IPB Satellite for Food Security and Environmental Monitoring

Preliminary study of bridge deformation monitoring using GPS and CRP (case study: Suramadu Bridge)

Hepi Hapsari Handayani*, Yuwono, Taufik M.

Geomatics Department Sepuluh Nopember Institut of Technology, ITS Sukolilo Campuss, Surabaya, 60111, Indonesia

Abstract

Deformation monitoring is one alternative methods that can become the indicators of brifge feasibility. The tools that can be applied for the deformation monitoring are GPS (Global Positioning System) technology and CRP (Close Range Photogrametry, since they are effective, easy, and can be used for multitemporal application. Suramadu bridge is a landmark building of East Java that is connecting Java and Madura islands. This objective of this study is to determine the deflection of Suramadu bridge.

Global Positioning System (GPS) were employed to monitor the deflection in the middle of bridge by kinematic methods using precise ephemeris data for correcting coordinate. For the entire span bridge, CRP method is applied using a non-metric camera with self callibration and space resection processing in bundle adjustment technique.

The results are still preliminary views, and at the moment this study is still underway. Based on these preliminary results, it appears that there are deflection in both horizontal and vertical axes based on 3 times of observation. Using CRP, the largest horizontal deformation inclined to the east at 80 mm and a decline of 12 mm. Using CRP, the smallest horizontal deformation is about 1 mm to the east and no change to the Z axis. The next stage for the study consists of CRP entire span bridge, GPS mid-span bridge (4 points), and modeling deformation.

© 2015 The Authors. Published by Elsevier B.V This is an open access article under the CC BY-NC-ND license

(<http://creativecommons.org/licenses/by-nc-nd/4.0/>).

Selection and peer-review under responsibility of the LISAT-FSEM Symposium Committee

Keywords: GPS, CRP, bridge deformation

1. Introduction

Suramadu Bridge is a landmark of East Java Province that is connecting the island of Java (in Surabaya) and Madura (in Bangkalan, exactly east Kamal). The major purpose of Suramadu's establishment is to accelerate

* Hepi Hapsari Handayani. Tel.: +62-31-5929486-7 fax: +62-31-5929487

E-mail address: hapsari@geodesy.its.ac.id

development and economic infrastructure on Madura Island. Suramadu is the longest bridge in Indonesia that has a length of 5438 m which was built with a large investment. In addition, it is expected to have a long life for 100 years. Thus, economic and population income, especially in Madura could be improved. The bridge is passed by around of 35,000 motorcycles and 23,000 cars per day, which in general are dominated by Madura's resident who taking business affairs in Surabaya [1]. With the main bridge structure which can be deflected, it is led to a decrease in the ability of the bridge. So the bridge health monitoring in this deformation, is vital in order to anticipate any existing conditions.

Traditionally, deformation monitoring techniques can be divided into geotechnical measurements and geomatics based surveys. Geotechnical measurements usually produce the amount of deformation relative to the reference mark on the actual object being monitored. The tools used are extensometers, tiltmeters, micrometer, etc. Thus, these measurements can only detect deformation in one-dimensional (1D), for example along the line. On the other hand, survey-based geomatics including traditional terrestrial survey with high precision levels, theodolites and electronic distance measurement (EDM) devices, global navigation satellite system (GNSS) [2] and remote sensing techniques including aerial photogrammetry [3] and terrestrial laser scanning [4, 5, 6]; and at close range photogrammetry [7, 8] can be used for the determination of deformation on an absolute scale, the measured points on the object of interest associated with other things belonging to the reference coordinate frame. Advantages of the deformation monitoring based geomatics survey is that the instruments used allows to detect deformation in three dimensional (3D). In addition, this method allows for redundant measurements, the precision can be evaluated with a rigorous adjustment. In addition to the advantages just described, the survey can also be automated based on geomatics [9]. This can reduce the effects of human error because of tedious job for repetitive inspections. Given the use of camera is cheap and easy, which increase in accuracy can be obtained from the application of analytic solutions geometrically, then the use of camera is one of the alternatives for the calculation of deformation. The use of a relatively inexpensive alternative method for monitoring bridge's deformation with digital photogrammetry is employing CRP (close range photogrammetry) technique by utilizing a DSLR (digital single lens reflect) camera. In the CRP technique, the quality of process for coordinates determination can be improved by convergent exposure to get redundant data or repetitive measurements.

Continuous data recording from the GPS satellites, using ground-based receivers and robust telemetry, can be used for monitoring the health of engineered structures, and can thereby be useful for assessing the public safety aspects of civil, structural, and earthquake engineering. Although the GPS system discussed here is not suitable for measuring displacements during seismic shaking (because we currently sample the GPS signals only once every 30 seconds), it is very well suited for measuring the static displacements of a structure within several hours after an earthquake. Since accelerometers cannot reliably recover static displacements and GPS cannot yet reliably recover strong ground motions, these instruments can only be seen as complementary devices. Real-time GPS systems capable of cm level precision at up to 10 Hz sampling rates presently exist, and we are currently evaluating them [10]. Such a system can also be used, of course, to examine a structure's response to other forces such as water loading, thermal effects, and wind, or to gradual changes in material or structural properties through time [11, 12, 13]. Objectives of this preliminary study are as follow :

- Determination of distortion in camera calibration process.
- Calculation for deformation of entire span bridge using CRP methods.
- Computation of deformation in mid-span bridge using GPS.

2. Methodology

This study is combining of GPS technology and digital photogrammetry. In this preliminary study, the method of digital photogrammetry is applied for measurement just in entire span bridge, while GPS is employed for measurement in mid-span bridge.

In CRP technique, the first step is to conduct camera callibration using a chessboard as callibration chart, as depicted in figure 1.

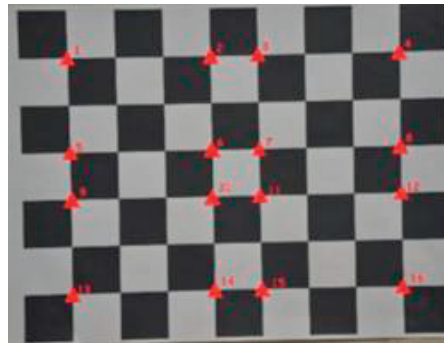


Fig. 1. Callibration chart

In the measurement using GPS techniques, GPS receiver antenna is placed in the fence on mid-span bridge, as presented in figure 2.

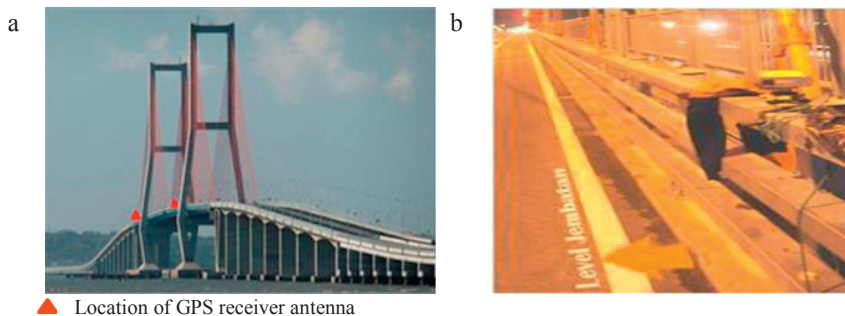


Fig.2.(a). Location of GPS receiver antenna, left receiver in Madura side, right receiver in Surabaya side; (b). GPS receiver antenna is installed in fence of the bridge

Equation for calculating deformation is as presented below.

$$dp = r'p - rp = dp (Xp, Yp, Zp; t) \tag{1}$$

Where ,
 rp = position of particle P at time $t = 0$ (before deformation);
 in this study expressed as the mean position
 $r'p$ = position after deformation at $t > 0$

3. Results and Analysis

This section consists of two parts explaining CRP technique and GPS technique, which result of deformation's calculation is included on each technique.

3.1. CRP technique

In CRP technique, result and analysis discusses about camera callibration and bridge deformation itself.

3.11. Callibration camera

In this study, camera callibration applies self-calibration method, which is a bundle adjustment technique conducted simultaneously. Included in this technique, there is a space resection process using Ground Control Points (GCPs) obtained by terrestrial survey using Total Station instrument. The calibrated focal length began to appear stable in the fourth iteration. Furthermore, the orientation parameters used for further processing are interior and

exterior orientation parameters camera which is determined by the fifth iteration, since there is no significant different between the fourth result and the fifth ones. Interior Orientation Parameters (IOP) and Exterior Orientation Parameter are listed in table 1 and table 2. When camera is shooted, focal length camera is setted up on 50mm. Based on result of camera callibration with bundle adjustment shows that the calibrated focal length is 48,798 mm. This indicates that there is a significant change amount of 1,202 mm. Empirical results indicated that changes in the values of such highly are possible on non-metric cameras, where the geometric lens does not have a standard frame because of the absence of fiducial marks. Table 2 presents EOP value, which shows an unsignificant different between three rotation angles (ω , ϕ , κ).

Table 1. Interior Orientation Parameter (IOP)

X_0 (mm)	Y_0 (mm)	f (mm)	k_1	k_2	p_1	p_2
-0,568	-0,052	48,798	-0,000882	0,0000131	0,000567	0,000125

Table 2. Exterior Orientation Parameter (EOP)

ω (rad)	ϕ (rad)	κ (rad)	XL (mm)	YL (mm)	ZL (mm)
-0,02198	-0,02037	-0,02161	89,578	86,712	737,602

Based on the results of camera calibration, corrected values of image coordinates are obtained. To determine the accuracy of coordinates based on the calibration results, error rate was calculated reposing for coordinates of initial image of the corrected image coordinates. The error rate was commonly called the reprojection error. Value of reprojection error is corrected for image coordinates. The error and its vector are shown in figure 3 and table 3. Reprojection error shows that the range of values are from -0,41582 mm up to 0,59612 mm for x axes and -0,30539 mm up to 0,40016 mm for y axes. GCPs of position lying on far of the centre has a large shift tending to be more than 0,15 mm and vector to outwards. Meanwhile, for points in the middle of GCP, the shift tends to be small, under 0.1 mm and the direction of the shift is to the center. This indicates that the camera used has barrel distortion. Based on the results of the reprojection error, it can be analyzed that the point that were located away from center has larger error.

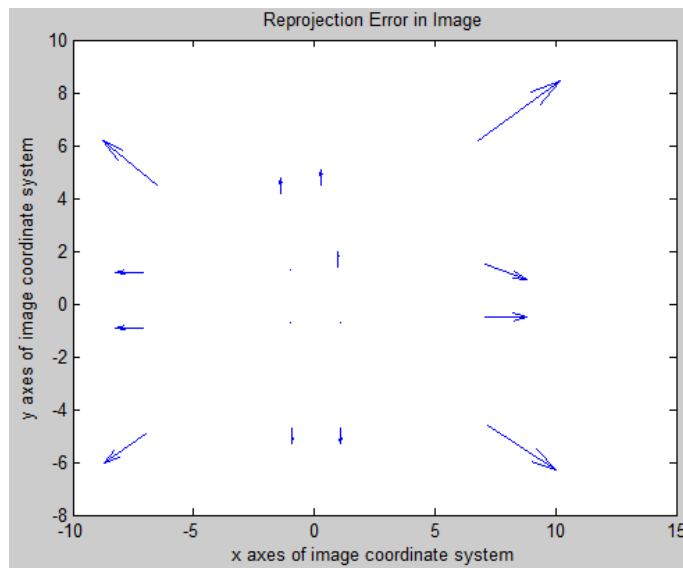


Fig.3. Reprojection error in image coordinate system

Table 3. Reprojection vector in image coordinate system

x(mm)	y(mm)
-0,41582	0,27231
-0,01798	0,11102
0,03501	0,10676
0,59612	0,40016
-0,23981	0,03498
-0,00398	-0,00012
0,01301	0,14001
0,33978	-0,08279
-0,22972	-0,01987
0,00311	0,00298
0,01617	0,00131
0,32789	-0,03087
-0,31978	-0,22897
-0,00102	-0,08712
0,04802	-0,09592
0,53997	-0,30539

As for the captured images on the edge in bridge spans at the both sides of Madura and Surabaya which are shown in figure 4 and figure 5 respectively, the images were mutually overlap one another, with a large patch that is at least 50%. Ground control points used in the images are the columns of the bridge.



Fig.4. Captured images overlapping one another of bridge spans in Surabaya side with distribution of GCPs (a). first image; (b). second image; (c). third image; (d). fourth image



Fig.5. Captured images overlapping one another of bridge spans in Madura side with distribution of GCPs (a). First image; (b). Second image (c). mosaicking of the first and second image.

3.1.2. Deformation by CRP

Deformation is calculated using GCPs which distribution presented in figure 5c. The point that have the largest deformation is 1a, which horizontal deformation towards to the northeast at 81mm and vertical deformation as 10 mm towards to upward. While, the point that have the smallest deformation is 5a, which the horizontal shift tends to the east about 1 mm and none vertical shift. For CRP result of deformation, mostly of vertical deformation directed upward. Deformation value of each point and vector of deformation is showed in table 4 and figure 6 respectively. Then, average of deformation is 0,038m with the standard deviation about 0,023m, as presented in table 5.

Table 4. Deformation horizontal and vertical per point

Point	Horizontal (X,Y)-mm	Vertical (Z)-mm
1a	81	10
1b	29	7
2a	22	8
2b	50	3
3a	10	15
3b	20	5
4a	31	6
4b	27	8
5a	2	0
5b	8	1
6a	67	0
6b	72	5
7a	39	1
7b	54	1

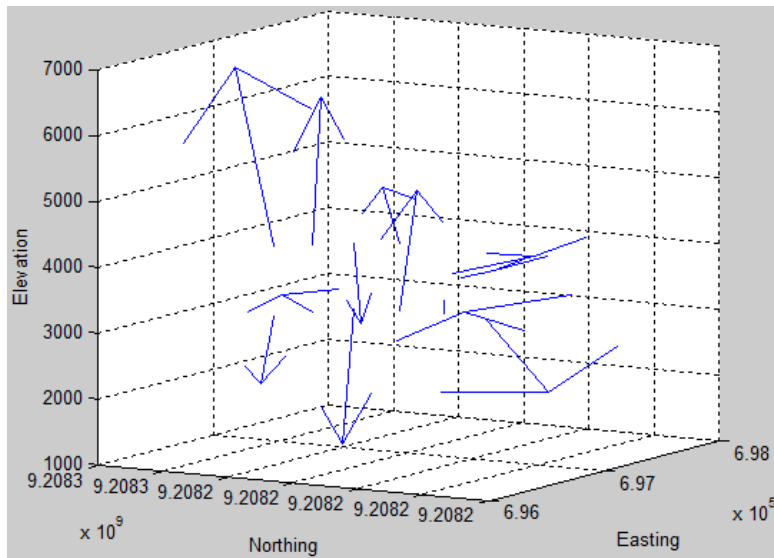


Fig.6. Vector of deformation

Table 5. Deformation value of GCPs

Point	Deformation (m)	Point	Deformation (m)
1a	0,082	1b	0.030
2a	0,023	2b	0,050
3a	0,018	3b	0,021
4a	0,032	4b	0,028
5a	0,002	5b	0,008
6a	0,067	6b	0,072
7a	0,039	7b	0,054
Average (m)		0,038	
Standard Deviation (m)		0,023	

The t test is employed to validate coordinate, it is for easting, northing, and elevation as presented in table 6, 7, and 8 respectively in below. The tables show that mostly the results of statistical test were accepted. However, there are some coordinates that do not meet the criteria of the statistical tests which were shown in the red font. Based on the statistical tests, we can conclude that the accuracy in X-axis direction is worse than the accuracy in Y axis and Z axis. Because most of the coordinates of CRP result was received in the student-t test statistics so there is no significant between the results of CRP and those of TS. For Easting coordinate, there are 4 points that are not accepted in statistical test because they are out of interval value.

Table 6. Result of t-student test for Easting coordinate

Point	TS (x)	Easting (m)	
		CRP1	CRP2
1a	696.769,531	696.769,352	696.769,421
1b	696.769,503	696.769,671	696.769,640
2a	696.769,295	696.769,325	696.769,310
2b	696.769,275	696.769,247	696.769,289
3a	696.768,838	696.768,830	696.768,982
3b	696.768,806	696.768,871	696.768,811
4a	696.768,325	696.768,304	696.768,331
4b	696.768,304	696.768,324	696.768,302

5a	696.767,825	696.767,820	696.767,817
5b	696.767,801	696.767,817	696.767,808
6a	696.767,464	696.767,424	696.767,474
6b	696.767,433	696.767,370	696.767,422
7a	696.766,708	696.766,773	696.766,742
7b	696.766,700	696.766,707	696.766,675

Based on table 7, the results presented that there is 1 point in Northing which was not passed on the statistical test. While in the Elevation test, all coordinate is accepted, which mean that they are satisfied, as listed in table 8.

Table 7. Result of t-student test for Northing coordinate

Point	TS (x)	Northing (m)	
		CRP1	CRP2
1a	9.208.256.671	9.208.256.539	9.208.256.569
1b	9.208.256.649	9.208.256.776	9.208.256.785
2a	9.208.250.739	9.208.250.747	9.208.250.740
2b	9.208.250.724	9.208.250.722	9.208.250.745
3a	9.208.244.292	9.208.244.289	9.208.244.287
3b	9.208.244.266	9.208.244.262	9.208.244.270
4a	9.208.237.304	9.208.237.294	9.208.237.307
4b	9.208.237.302	9.208.237.310	9.208.237.297
5a	9.208.230.445	9.208.230.447	9.208.230.447
5b	9.208.230.452	9.208.230.450	9.208.230.450
6a	9.208.223.812	9.208.223.841	9.208.223.807
6b	9.208.223.828	9.208.223.879	9.208.223.834
7a	9.208.218.097	9.208.218.037	9.208.218.059
7b	9.208.218.106	9.208.218.090	9.208.218.135

Table 8. Result of t-student test for Elevation

Point	TS (x)	Elevation (m)	
		CRP1	CRP2
1a	4.099	4.087	4.100
1b	3.027	3.025	3.020
2a	4.183	4.179	4.190
2b	3.156	3.154	3.155
3a	4.255	4.254	4.248
3b	3.242	3.251	3.241
4a	4.311	4.303	4.307
4b	3.292	3.293	3.302
5a	4.312	4.311	4.311
5b	3.302	3.304	3.305
6a	4.289	4.290	4.290
6b	3.263	3.268	3.263
7a	4.244	4.245	4.244
7b	3.166	3.166	3.167

3.2. GPS technique

This section consists of result of GPS measurement and deformation’s calculation.

3.2.1. GPS measurement

GPS data based on measurement of 2 epoch, date of measurements are presented in table 9 and coordinate of GPS base are showed in table 10. The standard deviation of measurement results is listed in table 11. Based on table 11, it shows that the second epoch is worse than the first epoch.

Table 9. Date of GPS measurement

No	Date	Total of Point	Start time	End time
1	April 17, 2014	2	14:08	22:00
2	May 16, 2014	2	13:51	21:45
3	June 13, 2014	2	10:15	21:30

Table 10. Coordinate of GPS base

Name	Latitude	Longitude	Ell.Height(m)
ITS CORS	7°16'47".95S	112°47'40".64E	47.951
KJSS02	7°12'31".31S	112°46'42".68E	34.383

Table 11. Coordinate of GPS base

No	Date	Std Dev N (m)	Std Dev E (m)
1	April 17, 2014	-0,0509	0,4871
2	May 16, 2014	-0,0176	0,5150

Based on 2 epochs of GPS measurements, bridge deflection is calculated as presented in table 12 and figure 7a for madura side. While for Surabaya side, results are listed in table 12 and showed in figure 7b. Based on the results, deflection deformation values in GPS of Madura side are obtained by calculating of average value of overall change in position. It is about 0,06036 m or 6,036 cm. Deformation values in GPS of Surabaya side are obtained by calculating the average value of overall change in position which is about 0,07004 m or 7,004 cm.

Table 12. Deflection of bridge in Surabaya and Madura side

Madura side	Surabaya side
Elevation's average (m)	72,43661
Standard deviation (m)	0,04425
Deformation (m)	-0,06036

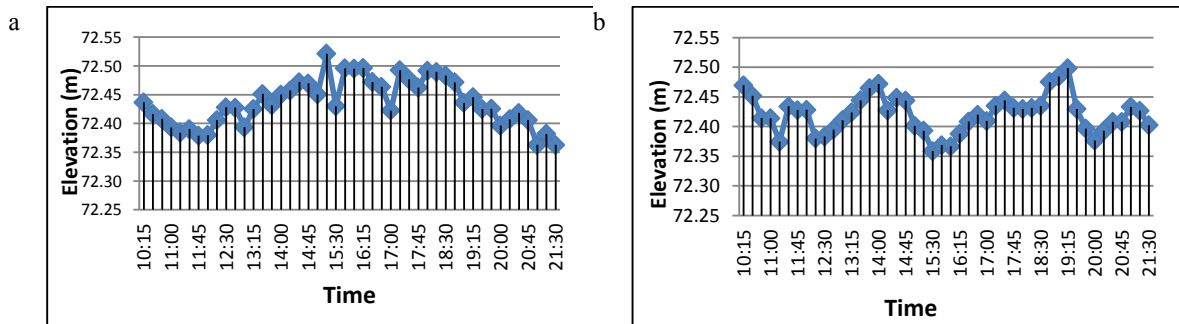


Fig.7. (a). Deflection in Madura side; (b). Deflection in Surabaya side

3.1.2. Deformation by GPS

Deformation based on GPS calculation is presented on table 13. Deformation was compared with the data of the quantity of vehicles passing the bridge, as showed in figure 8. The maximum deflection on upward movement of the GPS2 located on the side of Madura is 8,45455cm, with 255 motorcycles and 148 cars passing the bridge. The maximum deflection is directed downward which reached 7,38767cm, with 330 cars and 550 motorcycles. Based on the deflection data, it indicates that the longest bridge decreased by 0,00839 cm when first passenger car unit passed. While in Surabaya side, the maximum deflection on upward movement of the GPS3 is 7,75161cm, with 185 motorcycles and 86 cars. The maximum deflection on downward movement is 6.21950 cm, with 262 cars and 520 motorcycles. Based on the deflection data, it indicates that the longest bridge decreased by 0.00795cm cm when one passenger car unit passed.

Table 13. Deformation in vertical by GPS

Date	Point	Deformation (m)	Max-Deflection (cm)
June 13, 2014			8,45455
	GPS 2 (Madura)	-0,06036	-7,38767
	GPS 3 (Surabaya)	-0,07004	7,75161
			-6,21950

4. Conclusions

Conclusions of this paper are as follow.

1. Based on result of camera callibration with bundle adjustment, it shows that the calibrated focal length is 48,798mm. This indicates that there is a significant change of 1,202mm. Empirical results also indicate that changes in the value of such highly are possible in non-metric cameras, where the geometric lens does not have a standard frame because of the absence of fiducial marks. For rotation angles, there are no significant different between three rotation angles (ω , ϕ , κ).
2. Using CRP, the largest horizontal deformation is likely to the east of 80 mm and downwards at 12 mm, and the smallest horizontal deformation is likely to the east of 1 mm and none of vertical movement.
3. Using GPS, the maximum upward deflection of GPS2 (Madura) is 8.45455 cm and the maximum downward deflection is 7.38767cm. Using GPS, the maximum upward deflection of GPS3 (Surabaya) is 7.75161cm and the maximum downward deflection is 6.21950cm.

On going progress

1. CRP entire span bridge
2. GPS mid-span bridge(4 points)
3. Modeling deformation

Acknowledgements

Acknowledgement is for Higher Education Ministry of Indonesia for grant as Hibah Penelitian Unggulan Perguruan Tinggi.

References

1. (BPWS), B. P. (2013). Suramadu Report. Surabaya: www.bpws.go.id.
2. Baltasvias, E.P., Favey, E., Bauder, A., Bösch, H. and Pateraki, M. (2001). Digital Surface Modelling by Airborne. Photogrammetric Record, 17(98), 243-273.
3. Bond, J., Chrzanowski, A. and Kim, D. (2008). Bringing GPS into harsh environments for fully automated. GPS Solutions, 12(1), 1-11.
4. Celebi, M., W. Prescott, R. Stein, K. Hudnut, J. Behr and S. Wilson. (1998). GPS Monitoring of structures: recent advances. submitted to Earthquake Spectra.
5. DeLoach, S. R. (1989). Continuous Deformation Monitoring with GPS. Journal of Surveying Engineering, 115(1), 93-110.
6. Fraser, C.S. and Riedel, B. (2000). Monitoring the thermal deformation of steel beams via vision metrology. ISPRS, 268-276.
7. González-Auilera, D., Gómez-Lahoz, J. and Sánchez, J. (2008). A New Approach for Structural Monitoring of Large. Sensors, 8(8), 5866-5883.
8. Gordon, S.J. and Lichti, D.D. (2007). Modeling Terrestrial Laser Scanner Data for Precise Structural Deformation. Journal of Surveying Engineering, 133(2), 72-80.
9. Kim D., Langley R.B., Bond J., and Chrzanowski A. (2003). Local deformation monitoring using GPS in an open. GPS Solutions, 7(3), 176-185.
10. Lovse, J.W., Teskey, W.F., Lachapelle, G. and Cannon, M.E. (1995). Dynamic Deformation Monitoring of Tall. Journal of Surveying Engineering, 121(1), 35-40.

11. Maas, H.-G. and Hampel, U. (2006). Photogrammetric Techniques in Civil Engineering Material Testing and Structure Monitoring. *Photogrammetric Engineering & Remote Sensing*, 72(1), 39-45.
12. Monserrat, O. and Crosetto. (2008). Deformation measurement using terrestrial laser scanning data and least. *ISPRS Journal of Photogrammetry & Remote Sensing*, 63(2008), 142-154.
13. Nababan, P. (2008). *Structural Health Monitoring System*. Surabaya: Ministry of Public Works.